

Generation and application of the twisted beam with orbital angular momentum

Mingwei Gao (高明伟), Chunqing Gao (高春清), and Zhifeng Lin (林志锋)

Department of Opto-Electronics Engineering, Beijing Institute of Technology, Beijing 100081

Received August 14, 2006

The twisted Laguerre-Gaussian beam was generated by transforming of Hermite-Gaussian beams through an optical system consisting of three rotated cylindrical lenses. The intensity distribution and phase structure of the twisted hollow beam were theoretically analyzed by using Collins diffraction integral. By utilizing the method of mode decomposition, the theory of transformation was analyzed. In the experiment, micro particles were trapped and rotated by this twisted beam.

OCIS codes: 140.3460, 260.2110, 140.3300.

It is well known from Maxwell's theory that the electromagnetic field has linear momentum and angular momentum. The mechanical property of momentum was identified by Poynting vector^[1]. Circularly polarized beam has angular momentum, which is related to the spin of the photon. It was firstly demonstrated by Beth who observed the torque that exerted on half wave plate when a circularly polarized beam passed it^[2]. But it is less well known that the light might also have orbital angular momentum, related to the dislocation of phase front. In 1992, Allen *et al.* firstly predicted that the Laguerre-Gaussian mode had orbital angular momentum^[3]. The angular momentum has shown to have a good prospect in biology, atomic physics, and photon communication^[4–10]. In this paper, we present the results on the transforming of the unpolarized Hermite-Gaussian beams into Laguerre-Gaussian beams by using three rotated cylindrical lenses. By utilizing the method of mode decomposition, the theory of transformation was analyzed. In the experiment, the twisted beam with orbital angular momentum was obtained and used in trapping and rotating particles with dimension around 10 μm .

It is now well established that the beams with the azimuthal phase term $\exp(il\phi)$ such as linearly polarized Laguerre-Gaussian modes have an orbital angular momentum of $l\eta$ per photon^[3]. Figure 1 shows the intensity distribution and the phase front of the Laguerre-Gaussian beams.

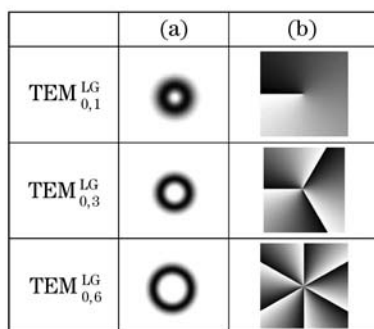


Fig. 1. Intensity distribution and phase distribution of the twisted Laguerre-Gaussian beams.

The Laguerre-Gaussian modes could be generated from the laser resonator directly, but for the reason of the inherent astigmatism of the resonator it is difficult to get a stable beam output. The common way is to generate the Laguerre-Gaussian beams by transforming the Hermite-Gaussian beam that is easily obtained by laser systems. An astigmatic optical element, such as a cylindrical lens, can be used to realize such transformation. A rotated cylindrical system is used to transform the Hermite-Gaussian beam into the Laguerre-Gaussian beam^[11,12]. It consists of three rotated cylindrical lenses with the focal lengths of $f/2$, f , and $f/2$. The axis of the cylindrical lens is rotated by 45° with respect to the axis of the input beam. The schematic diagram of the optical system is shown in Fig. 2.

When a Hermite-Gaussian beam $\text{TEM}_{m,0}^{\text{HG}}$ propagates through the three-lens system, the field of the output beam can be evaluated by using the Collins diffraction integral as^[13]

$$E_{\text{out}}(x_2, y_2) = \sqrt{\frac{-ik}{2\pi f}} \iint E_{\text{in}}(x_1, y_1) \times \exp\left(-\frac{ik}{f\sqrt{2}}x_2(x_1 + y_1)\right) \times \delta\left(y_2 + \frac{1}{\sqrt{2}}(-x_1 + y_1)\right) dx_1 dy_1, \quad (1)$$

where $E_{\text{out}}(x_2, y_2)$ describes the output field in the principal coordinates of the transformation optics, $E_{\text{in}}(x_1, y_1)$

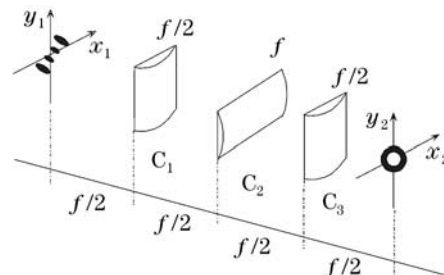

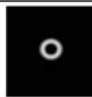




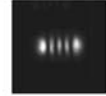



Fig. 2. Three rotated cylindrical lenses used for generating the twisted hollow beam.

Table 1. Results of the Theoretical Calculation and Experiment

	TEM _{2,0} ^{HG}	TEM _{2,0} ^{LG}	TEM _{4,0} ^{HG}	TEM _{4,0} ^{LG}
	Input Beam	Output Beam	Input Beam	Output Beam
Theoretical Calculation				
Measurement Results				

is the field of the input Hermite-Gaussian beam TEM_{*m*,0}^{HG} which is given by^[14]

$$\text{TEM}_{m,0}^{\text{HG}}(x_1, y_1) = \sqrt{\frac{2}{\pi}} \cdot \frac{E_0}{\sqrt{2^m m!} w_0} H_m \left(\frac{\sqrt{2} x_1}{w_0} \right) \times \exp \left(-\frac{x_1^2 + y_1^2}{w_0^2} \right), \quad (m \geq 1). \quad (2)$$

The focal lengths of the cylindrical lenses are chosen to match the Rayleigh lengths z_{R_x} , z_{R_y} of the input beam,

$$f = z_{R_x} = z_{R_y} = \pi w_0^2 / \lambda. \quad (3)$$

Substituting Eqs. (2) and (3) into Eq. (1), the field of the output beam can be obtained. In the focal plane of the cylindrical lens C₃, the field of the output beam is

$$E_{\text{out}}(x_2, y_2) = \frac{E_0}{w_0} \sqrt{\frac{-i}{\pi}} \cdot \frac{2^{m/2}}{\sqrt{m!}} \left(\frac{i x_2 - y_2}{w_0} \right)^m \times \exp \left\{ -\frac{x_2^2 + y_2^2}{w_0^2} \right\}. \quad (4)$$

In polar coordinates Eq. (4) becomes

$$E_{\text{out}}(r_2, \varphi_2) = \frac{E_0}{w_0} \sqrt{\frac{-i}{\pi \cdot m!}} \cdot \left(\frac{\sqrt{2} i r_2}{w_0} \right)^m \times \exp \left\{ -\frac{r_2^2}{w_0^2} \right\} \exp \{-i m \varphi_2\}. \quad (5)$$

The output beam is a Laguerre-Gaussian beam of the order 0, m . Table 1 shows the theoretical calculation and experimental results of the transformation of TEM_{2,0}^{HG} and TEM_{4,0}^{HG}.

The Laguerre-Gaussian modes and Hermite-Gaussian modes both form the complete, orthogonal basic set of resonator eigen functions. Any coherent field distribution can be described by a set of Laguerre-Gaussian modes or Hermite-Gaussian modes. It means that the Laguerre-Gaussian mode can be decomposed into a set of Hermite-Gaussian modes and *vice versa*. By using the relation between the Laguerre and the Hermite polynomials, a Laguerre-Gaussian mode can be decomposed into a set of Hermite-Gaussian modes of same order^[15]

$$\text{TEM}_{mn}^{\text{LG}}(x, y, z) = \sum_{k=0}^N i^k a(n, m, k) \text{TEM}_{N-k,k}^{\text{HG}}(x, y, z), \quad (6)$$

where

$$a(n, m, k) = \left(\frac{(N-k)! k!}{2^N n! m!} \right) \cdot \frac{1}{k!} \cdot \frac{d^k}{dt^k} [(1-t)^n (1+t)^m] |_{t=0}, \quad N = n + m.$$

Since i means a $\pi/2$ phase difference, the factor i^k in the Eq. (6) corresponds to a $\pi/2$ phase difference between the successive components. If the principal axis has an angle of $\pi/4$ with the coordinate axis, the decomposition reads^[15]

$$\text{TEM}_{mn}^{\text{HG}} \left(\frac{x+y}{\sqrt{2}}, \frac{x-y}{\sqrt{2}}, z \right) = \sum_{k=0}^N a(n, m, k) \text{TEM}_{N-k,k}^{\text{HG}}(x, y, z). \quad (7)$$

Figure 3 shows the examples of beam decomposition.

Comparison of Eqs. (6) and (7) shows that they are almost the same except of a factor i^k or a phase shift of $\pi/2$ between two adjacent components. When a 45° rotated Hermite-Gaussian beam passes through this optical system, which causes a $\pi/2$ phase difference between the adjacent components, the output beam will be a Laguerre-Gaussian beam. For a stigmatic Gaussian beam the Gouy shift is given by^[14] $(n+m+1)\phi(z)$. For an astigmatic beam the Gouy shift has two contribution^[16]: $(n+1/2)\phi_x(z) + (m+1/2)\phi_y(z)$, with

$$\begin{aligned} \phi_x(z) &= a \tan((z - z_{0x}) / z_{R_x}), \\ \phi_y(z) &= a \tan((z - z_{0y}) / z_{R_y}). \end{aligned} \quad (8)$$

When the rotated Hermite-Gaussian beam propagates through the rotated cylindrical system, the Gouy shift of adjacent components reads

$$\begin{aligned} \Delta\phi &= [(n+1/2)\phi_x(z) + (m+1/2)\phi_y(z)] \\ &\quad - [((n+1)+1/2)\phi_x(z) + ((m-1)+1/2)\phi_y(z)] \\ &= \phi_y(z) - \phi_x(z). \end{aligned} \quad (9)$$

Figure 4 shows the beam propagation through the

$$\begin{aligned} \text{HG} &= \text{HG} + \text{HG} + \text{HG} \\ \text{LG} &= \text{HG} + i \text{HG} + i^2 \text{HG} \end{aligned}$$

Fig. 3. Decomposition of Laguerre-Gaussian mode TEM_{2,0}^{LG} and Hermite-Gaussian mode TEM_{2,0}^{HG} into a set of Hermite-Gaussian modes with same order.

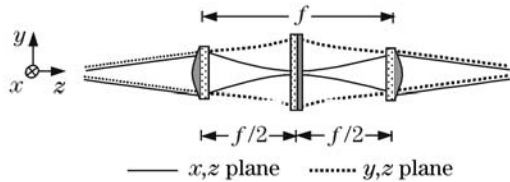


Fig. 4. A beam propagating through the rotated cylindrical lens system.

rotated cylindrical lens system. The solid lines denote the beam in the x,z plane, and the dashed lines in the y,z plane.

Substituting Eq. (8) into Eq. (9) delivers

$$\Delta\phi = 2 \cdot a \tan\left(\frac{f}{2 \cdot z'_{Ry}}\right) - 2 \left(a \tan\left(\frac{f}{z_{Rx}}\right) - a \tan\left(\frac{f}{2 \cdot z_{Rx}}\right) \right), \quad (10)$$

where z_{Rx} is the Rayleigh length in the x,z plane, $z_{Ry} = z_{Rx} = f$, z'_{Ry} is the Rayleigh length after the cylindrical lens C_1 in the y,z plane,

$$z'_{Ry} = \frac{z_{Ry} \cdot (f/2)^2}{z_{Ry}^2 + (z - f/2)^2}, \quad (11)$$

where $z = f/2$. Substituting it into Eq. (9) yields

$$\Delta\phi = \phi_y(z) - \phi_x(z) = \frac{\pi}{2}. \quad (12)$$

Similar to the “ $\pi/2$ ” waveplate, we will call the three-lens system a “ $\pi/2$ ” mode converter. The transformation can be reversed. When a Laguerre-Gaussian beam passing through such a converter, the output beam will be Hermite-Gaussian beam. The three rotated cylindrical lenses system can be simplified into a two cylindrical lenses system firstly used by Tamm *et al.*^[17]. Similar to the “ π ” waveplate, there should be a “ π ” mode converter to transform the left-hand Laguerre-Gaussian beam into right-hand Laguerre-Gaussian beam or *vice versa*. A Dove prism is commonly used to realize such transformation. The Collins integral of Dove prism can be written as^[13]

$$E_2(x_2, y_2) = \frac{1}{\sqrt{\det(A)}} \times \iint E_1(x_1, y_1) \delta(\vec{r}_1 + A \cdot \vec{r}_2) dx_1 dy_1. \quad (13)$$

Substituting Eq. (2) into Eq. (13) delivers

$$E_2(x_2, y_2) = \frac{E_0}{w_0} \sqrt{\frac{-i}{\pi}} \cdot \frac{2^{m/2}}{\sqrt{m!}} \left(\frac{ix_2 + y_2}{w_0} \right)^m \times \exp\left\{ -\frac{x_2^2 + y_2^2}{w_0^2} \right\}. \quad (14)$$

In polar coordinates Eq. (14) can be written as

$$E_{out}(r_2, \varphi_2) = \frac{E_0}{w_0} \sqrt{\frac{-i}{\pi \cdot m!}} \cdot \left(\frac{\sqrt{2}ir_2}{w_0} \right)^m \exp\left\{ -\frac{r_2^2}{w_0^2} \right\} \times \exp\{im\varphi_2\}. \quad (15)$$

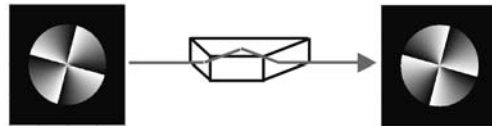


Fig. 5. Shift of the phase front when a Laguerre-Gaussian beam passes through the Dove prism.

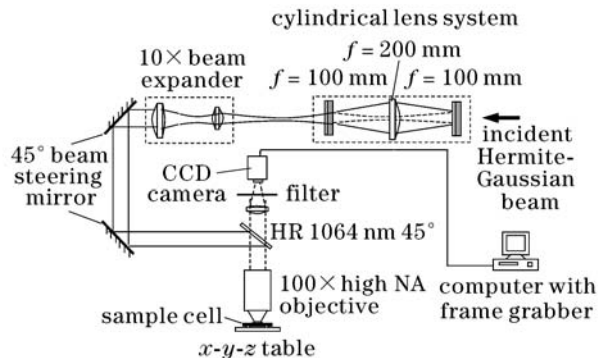


Fig. 6. Experimental setup of using the twisted hollow beam for rotating particles.

Comparing Eq. (5) with Eq. (15), we find that the direction of the phase front is reversed, which means that the left-hand Laguerre-Gaussian beam is transformed into right-hand Laguerre-Gaussian beam and *vice versa*. In Fig. 5, it can be seen that the phase front is reversed when the beam passes through the Dove prism.

Since the twisted Laguerre-Gaussian beam has an orbital angular momentum, which is transferable to absorbing sample, it can be used to trap and rotate micro particles. Figure 6 shows the experimental setup. The Hermite-Gaussian beam $TEM_{2,0}^{HG}$ generated from a diode pumped Nd:YAG mode generator^[18] with an output wavelength of 1064 nm was transformed into Laguerre-Gaussian beam through the three cylindrical lenses system shown in Fig. 2. For reducing the beam divergence, a 10 \times telescope was used before the twisted hollow beam entered the microscope. Then the beam propagated through two 45 $^\circ$ high-reflection steering mirrors and a 100 \times oil-immersed objective with a numerical aperture (NA) of 1.25. The dye particle with a dimension of around 10 μm was used in the experiment. Figure 7 shows the images of the particle with a rotation frequency of 3.8 Hz. The power of input beam $TEM_{2,0}^{LG}$ was 60 mW. The frequency of particle rotation increased with the power and the mode number of the input Laguerre-Gaussian beam. Figure 8 shows the dependence of the angular speed of rotation on the power of the beam.

When the three cylindrical lenses were rotated from 45 $^\circ$ with respect to the axis of input beam to 135 $^\circ$, the reverse rotation of micro particle was observed. Since the spin angular momentum and scattering force are independent of the direction of the cylindrical lens, it is

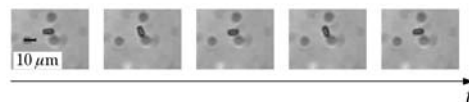


Fig. 7. Rotation of the particle. The frequency of rotation is about 3.8 Hz.

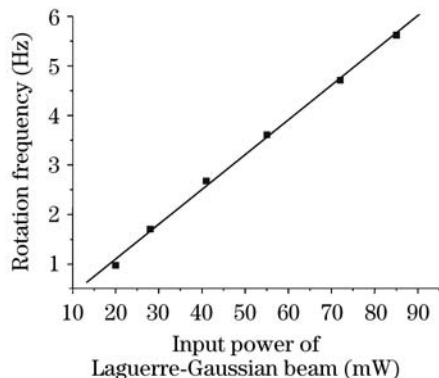


Fig. 8. Rotation frequency versus the power of the input beam.

testified that the rotation of the particle is caused by the orbital angular momentum.

In steady state, the torque of field is balanced by the torque of the liquid, which delivers the stationary angular velocity. The torque transferred to the particles can be given by

$$\tau = j_{Z,L} \eta_{\text{abs}} = \frac{\lambda m P}{2\pi c} \cdot \eta_{\text{abs}}, \quad (16)$$

where η_{abs} is the absorption coefficient of the particle. For a torque τ , the limited angular velocity of the particle with a radius r is

$$\omega_{\text{lim}} = \frac{\tau}{-8\pi \cdot r^3 \cdot \eta_{\text{liquid}}}, \quad (17)$$

where η_{liquid} is the viscosity of the surrounding liquid. For a particle with a dimension around $10 \mu\text{m}$ and an input power of 60 mW , the rotation speed is about 4 Hz , which implies that the absorption of the particle is of the order of 9% .

The Laguerre-Gaussian beam was generated by propagating the Hermite-Gaussian beam through the three rotated cylindrical lenses system. The generated beam has a ring intensity distribution and a twist phase distribution that is related to the orbital angular momentum. The twisted beam was used in trapping and rotating micro particles.

This work was partly supported by the National Natural Science Foundation of China (No. 69908001), and

the Characterization of Optical Components and Laser Beams II of Germany and the international cooperation agreed by DFG and NSFC. Prof. G. Wei, Dr. B. Eppich, Dipl. Phys. G. Mann are greatly grateful for their fruitful discussions and helps. M. Gao's e-mail address is ghew@bit.edu.cn.

References

1. J. D. Jackson, *Classical Electrodynamics* (Wiley, New York, 1962).
2. R. A. Beth, *Phys. Rev.* **50**, 115 (1936).
3. L. Allen, M. W. Beijersbergen, and R. J. C. Spreeuw, *Phys. Rev. A* **45**, 8185 (1992).
4. H. He, M. E. J. Friese, N. R. Heckenberg, and H. Rubinsztein-Dunlop, *Phys. Rev. Lett.* **75**, 826 (1995).
5. M. E. J. Friese, J. Enger, H. Rubinsztein-Dunlop, and N. R. Heckenberg, *Phys. Rev. A* **54**, 1593 (1996).
6. T. Kuga, Y. Torii, N. Shiokawa, T. Hirano, Y. Shimizu, and H. Sasada, *Phys. Rev. Lett.* **78**, 4713 (1997).
7. B. Xia and W. Hai, *Chin. Opt. Lett.* **3**, 373 (2005).
8. M. P. MacDonald, G. C. Spalding, and K. Dholakia, *Nature* **426**, 421 (2003).
9. J. Leach, M. J. Padgett, S. M. Barnett, S. Franke-Arnold, and J. Courtial, *Phys. Rev. Lett.* **88**, 257901 (2002).
10. J. Leach, J. Courtial, K. Skeldon, S. M. Barnett, S. Franke-Arnold, and M. J. Padgett, *Phys. Rev. Lett.* **92**, 013601 (2004).
11. A. T. Friberg, E. Tervonen, and J. Turunen, *J. Opt. Soc. Am. A* **11**, 1818 (1994).
12. A. Friberg, C. Gao, B. Eppich, and H. Weber, *Proc. SPIE* **3110**, 317 (1997).
13. N. Hodgson and H. Weber, *Optical Resonators: Fundamentals, Advanced Concepts and Applications* (Springer Verlag, Berlin, 1997).
14. A. E. Siegman, *Laser* (University Science Books, Mill Valley, 1986).
15. E. Abramochkin and V. Volostnikov, *Opt. Commun.* **83**, 123 (1991).
16. D. C. Hanna, *IEEE J. Quantum Electron.* **5**, 483 (1969).
17. C. Tamm and C. O. Weiss, *J. Opt. Soc. Am. B* **7**, 1034 (1990).
18. H. Laabs and B. Ozygus, *Opt. Laser Technol.* **28**, 213 (1996).